

Short Communication

# Dynamic characteristics of inertial actuator featuring piezoelectric materials: Experimental verification

S.B. Choi\*, S.R. Hong, Y.M. Han

*Department of Mechanical Engineering, Smart Structures and Systems Laboratory, Inha University, Incheon 402-751, Republic of Korea*

Received 26 April 2006; received in revised form 23 November 2006; accepted 16 January 2007

Available online 27 February 2007

---

## Abstract

This paper presents dynamic characteristics of a novel type of inertial actuator featuring piezoelectric materials for a mount system. As a first step, the piezoceramic stack is devised and its force and displacement characteristics are experimentally investigated with respect to the applied voltage. Subsequently, a new type of inertial actuator is constructed and its dynamic model is derived. The effectiveness of the model is then verified through comparison of voltage-dependent actuating forces between experiment and analysis. In addition, actuating force of the proposed inertial actuator is identified with respect to the applied voltage.

© 2007 Elsevier Ltd. All rights reserved.

---

## 1. Introduction

Recently, smart material actuators such as piezoelectric material, shape memory alloy and electro-rheological fluid are widely used for effective vibration control of flexible structures [1–3]. Among these, the piezoelectric material is the most promising candidate since it features fast response time and easy controllability. When the piezoelectric material is used for vibration control, there are basically two approaches. One approach is to directly bond the piezoactuator on the structures. This method is simple to fabricate and effective for the small-sized structures, which have high flexibility [4–6]. The other approach is to use active mount (or isolator), which can be fabricated using the piezoelectric actuator and rubber element, and applied to the vibration control systems. This method is complicated, but very effective for the large-sized flexible structures [7,8].

The active mount featuring the piezoelectric elements can be classified into two types: parallel type and serial type. The parallel type uses an active piezoelectric element placed between the vibration source and receiver (base) [9,10]. This type is very useful for the control of vibration source, and requires small stiffness of the active element. The serial type uses active piezoelectric elements placed between the vibration source and intermediate mass [11,12]. This type is also useful for the control of vibration source in discrete vibrating systems and needs appropriate weight on controls of vibrating source or force transmission to the base

---

\*Corresponding author. Tel.: +82 32 860 7319; fax: +82 32 868 1716.

E-mail address: [seungbok@inha.ac.kr](mailto:seungbok@inha.ac.kr) (S.B. Choi).

URL: <http://www.ssslslab.com>.

structure. Even though these two types of active mounts are widely used for vibration control of various dynamic systems, alternative means of active mounts need to be devised by adopting inertial actuator [13] in order to achieve successful vibration control of flexible structures instead of the vibration source.

The main contribution of this work is to propose a new type of inertial piezostack actuator, which can be adapted to an inertial type of mount, and experimentally identified its dynamic characteristic. The proposed inertial actuator consists of top inertial mass, pre-stress spring and piezoelectric element. After constructing the piezoceramic stack, the relationship between actuating force and applied voltage is derived. In addition, the voltage-dependent displacement is experimentally identified with respect to the exciting frequency. Subsequently, a new type of inertial actuator is constructed and its dynamic model is derived. The effectiveness of the model is then verified through comparison of voltage-dependent actuating forces between experiment and mathematical model.

## 2. Piezoceramic stack

In phenomenological terms, the piezoelectricity is described as coupling between a quasi-static electric field and dynamic mechanical motion. The direct and converse piezoelectric effects have been treated as reversible. The linear constitutive relations of the piezoelectric materials are typically represented in a matrix notation as follows [6,7]:

$$S_p = s_{pq}^E T_q + d_{kp} E_k, \quad (1)$$

$$D_i = d_{iq} T_q + \varepsilon_{ik}^T E_k. \quad (2)$$

In the above,  $S$  is the strain tensor,  $S^E$  is the elastic compliance matrix when subjected to a constant electrical field,  $T$  is the stress tensor,  $d$  is the matrix of piezoelectric charge constants,  $D$  is the electric displacement tensor, and  $\varepsilon^T$  is the permittivity measured at a constant stress. These equations essentially state that the material strain and electrical displacement exhibited by the piezoelectric material are both linearly affected by the mechanical stress and electrical field to which the piezoelectric material is subjected.

The electromechanical behavior of the piezoceramic actuator (or piezoelectric stack actuator), providing actuation along the polarized direction, can be expressed as follows:

$$S_3 = s_{33}^E T_3 + d_{33} E_3, \quad (3)$$

$$D_3 = d_{33} T_3 + \varepsilon_{33}^T E_3. \quad (4)$$

Thus, the constitutive equation of the piezoceramic actuator, stacked by  $n$  piezoelectric layers, can be derived as follows:

$$\begin{aligned} F_p(t) &= AT_3 = \frac{A}{s_{33}} S_{33} - \frac{Ad_{33}}{s_{33}} E_3 \\ &= \frac{A}{s_{33}} \frac{\delta(t)}{l} - \frac{nAd_{33}}{s_{33}} \frac{V_p(t)}{l} \\ &= K_p \delta(t) - \alpha_p V_p(t) = K_p \delta(t) - F_a(t). \end{aligned} \quad (5)$$

In the above,  $F_p(t)$  is the load applied to the piezoceramic actuator,  $A$  is the cross-sectional area of the piezoelectric ceramic element.  $l$  and  $\delta(t)$  are the length and stroke of the piezoceramic actuator, and  $F_a(t)$  is the force exerted by the electric voltage  $V_p(t)$ .  $K_p (= A/s_{33}l)$  is the spring rate,  $\alpha_p (= Ad_{33}n/s_{33}l)$  is the proportional constant which is related to the total stack capacitance  $C$  as follows [14]:

$$\alpha_p = \frac{g_{33}C}{nS_{33}}, \quad (6)$$

where  $g_{33}$  is the matrix of piezoelectric voltage constants.

The schematic configuration and photograph of piezoceramic actuator devised in this work are shown in Fig. 1. For the piezostack 46 layers of bipolar piezoelectric ceramic disc with the thickness of 50  $\mu\text{m}$  are piled and pre-stressed by the preload spring. The elements of the piezoelectric ceramic discs are connected

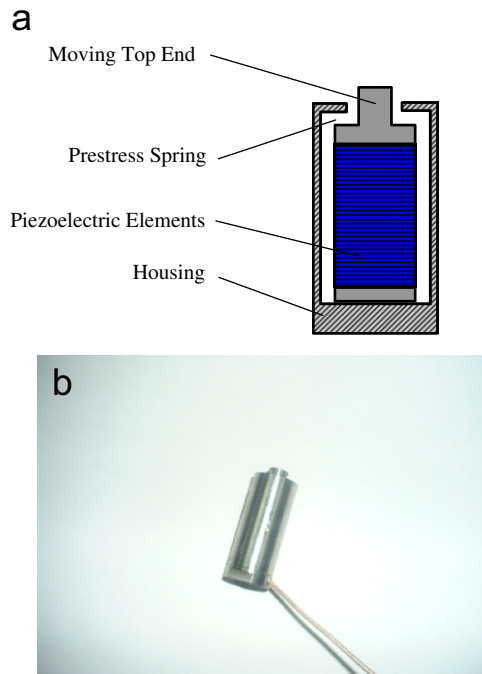


Fig. 1. Configuration of the piezoceramic stack: (a) schematic configuration and (b) photograph.

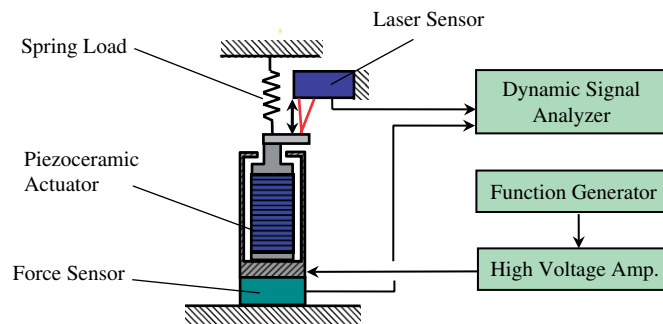


Fig. 2. Experimental setup for the force–displacement measurement.

electrically in parallel. The pre-stressing of the stack actuator improves the actuator performances, and also compensates the tensile stress to prevent damage of the piezoelectric ceramic discs. Furthermore, it increases the actuator stability against impact of bending or other non-axial forces. In this work, the preload imposed to the piezoceramic actuator is 300 N. The outer dimension of the piezoelectric stack and housing are  $D13 \times L36$  mm and  $D18 \times L51$  mm, respectively.

The basic performances of the piezoceramic actuator such as the displacement and force characteristics are investigated in the time and frequency domains. Fig. 2 presents the configuration of the experimental setup for the measurement of the displacement and force of the piezoceramic actuator. The piezoelectric stack is fixed to the base and activated by the voltage amplifier (Model 50/750, Trek, USA). The gain of voltage amplifier is set to be 20(V/V). The function generator (Model 178, Wavetek, USA) is used to provide the command signal input to the high-voltage amplifier. The displacement of the piezoelectric stack actuator is measured by the laser sensor (LC2430, Keyence, Japan), while the force is measured by the force transducer (Type 8200, B&K, Denmark). It is noted that the steel structure is used to apply the spring load to the piezoceramic stack actuator.

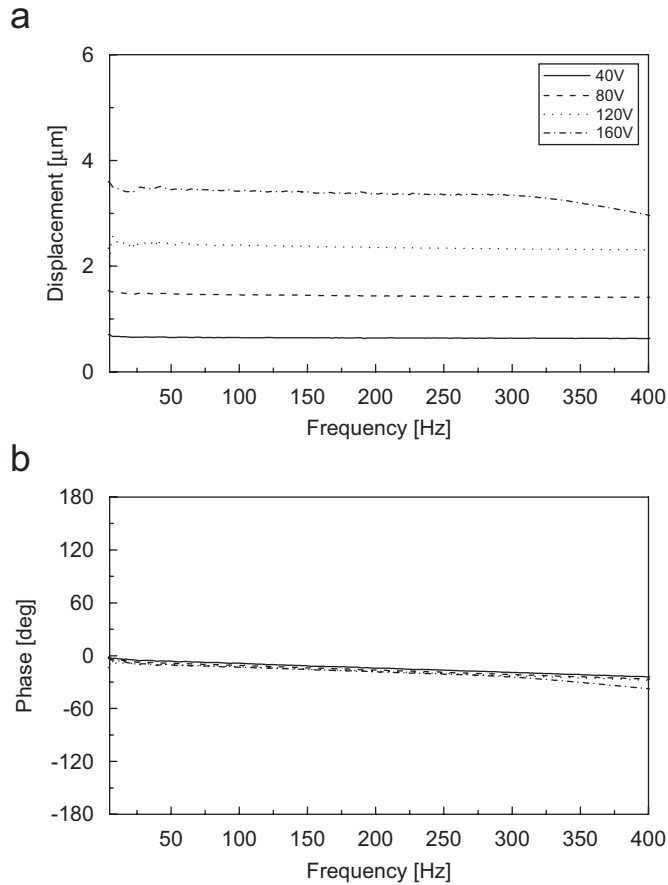


Fig. 3. Frequency responses of free-displacement of the piezoceramic actuator: (a) magnitude and (b) phase.

Fig. 3 presents the frequency response of the displacement of the piezoceramic actuator without mechanical load (or without the spring load). In other words, the displacement shown in Fig. 3 indicates the free-extension with various voltage magnitudes. It is clearly seen that the free-displacement is increased as the voltage increases. In addition, it is observed that the piezoceramic stack used in this work can produce the displacement of  $3.4\ \mu\text{m}$  by applying voltage of 160 V within the frequency range of 300 Hz. It is noted that the operating frequency is far below the first natural frequency of the actuator because the target mount system, which consists of the proposed inertial actuator, and rubber element operates at the frequency range of 300 Hz. Fig. 4(a) presents the time response of the piezoceramic actuator with the spring load. The sinusoidal voltage with frequency of 100 Hz is applied and the corresponding force is measured. The force is increased as the voltage increases, as expected. Fig. 4(b) presents the force vs. displacement diagram of the piezoelectric stack actuator. From the slope of the force vs. displacement, the averaged value of the stiffness is obtained by  $63\ \text{MN/m}$ . On the other hand, the voltage-dependent actuating force of the piezoceramic actuator  $F_a(t)$  can be obtained by adopting the value which intercepts the zero displacement. The actuating force of the piezoceramic actuator is evaluated by 220 N at the input voltage of 160 V.

### 3. Inertial actuator

In this work, a new type of inertial active actuator is devised utilizing the piezoceramic stack actuator. Fig. 5(a) shows the schematic configuration of the proposed inertial active actuator. The actuator consists of the inertial mass on the top of the piezoceramic stack, the pre-stress spring and the housing. The force, exerted by the piezoelectric effect, acts on the inertial mass and reacts to the opposite side of the piezoceramic

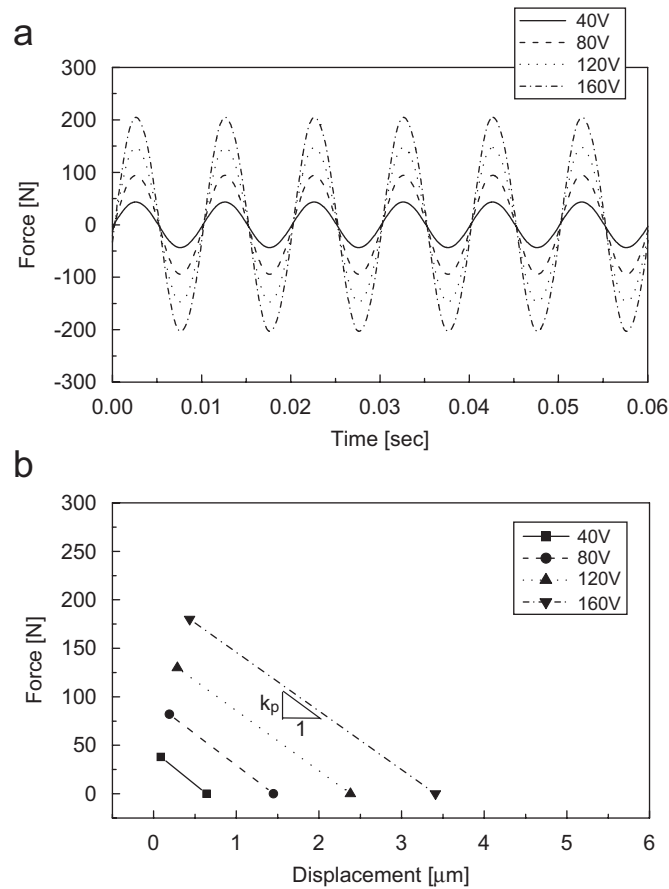


Fig. 4. Dynamic characteristic of the piezoceramic actuator under spring load (excitation frequency: 100 Hz): (a) force vs. time and (b) force vs. displacement.

actuator. Fig. 5(b) presents the mechanical model of the proposed inertial active actuator. From the mechanical model, the equation of motion of the inertial active actuator can be derived as follows.

$$m_I \ddot{y}_I(t) + c_p \dot{y}_I(t) + k_p y_I(t) + F_a(t) = 0, \tag{7}$$

$$F_i(t) = m_I \ddot{y}_I(t). \tag{8}$$

In the above equations,  $y_I$  is the displacement of the inertial mass  $m_I$ ,  $c_p$  is the damping constant, and  $F_i(t)$  is the inertial force. The weight of the inertial mass should be chosen by considering the control force requirement and modal characteristics of the flexible structure to be controlled. By incorporating the actuating force of the proposed piezoceramic actuator with the above equations, an appropriate size of the actuator has been fabricated as shown in Fig. 5(c). The inertial mass is set by 0.55 kg.

As a first step, in order to investigate the time delay due to the inertial mass the phase of the inertial force is measured and presented in Fig. 6. It is clearly observed that the proposed active actuator does not cause the time delay due to the inertial mass at various voltages. Fig. 7 presents the time response of the inertial force of the proposed active actuator. The sinusoidal voltage with the magnitude of 50 V is applied and the inertial force is measured from the force transducer. On the other hand, the inertial force is predicted from Eqs. (7) and (8) and compared with the measured one. It is clearly seen that the agreement between the experiment and prediction from the model is favorable. The inertial force is also identified as a function of exciting frequency and presented in Fig. 8. As expected from Eqs. (7) and (8), the inertial force is increased as the frequency increases with the same applied voltage. It is also observed that the proposed model fairly well predicts the measured inertial force.

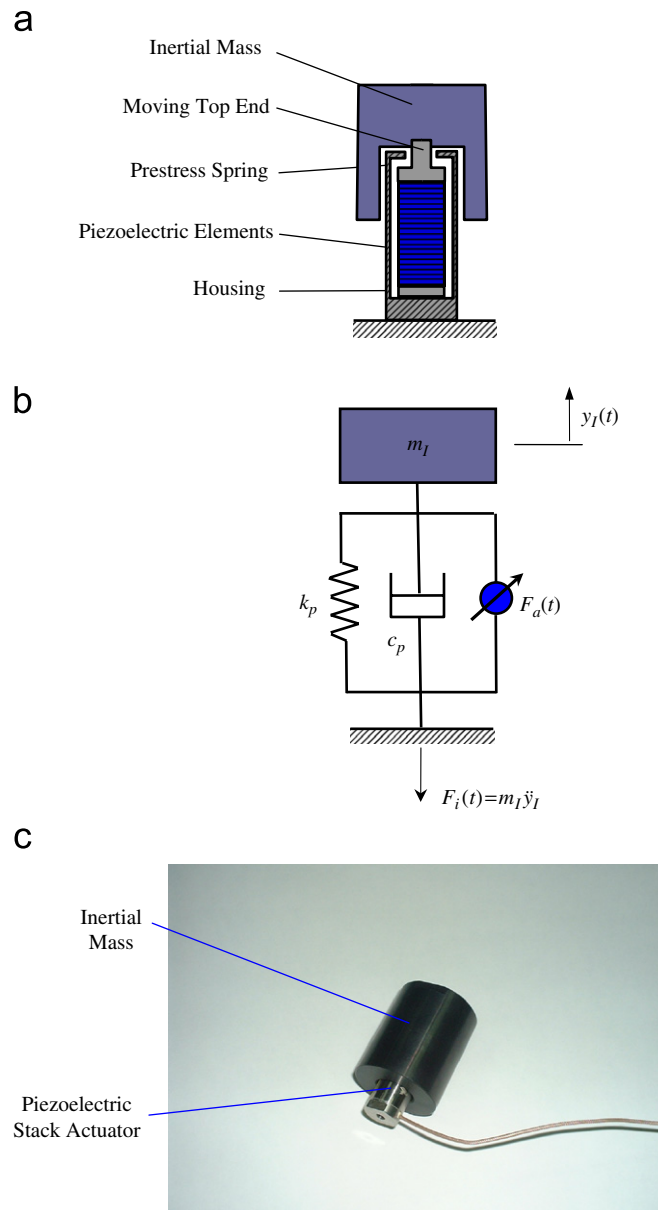


Fig. 5. Schematic configuration and mechanical model of the inertial type actuator: (a) schematic configuration, (b) mechanical model and (c) photograph.

Fig. 9 presents the identified actuating force exerted by the proposed inertial actuator featuring the piezoceramic stack actuator. The actuating force,  $F_a(t)$ , can be expressed as a linear function. But for the better identification of the actuation force, an exponential function of the input voltage is adopted as follows:

$$F_a(t) = \alpha_1 (V_p(t))^{\alpha_2} N. \quad (9)$$

In the above equation, the proportional coefficient  $\alpha_1$  and exponent  $\alpha_2$  are identified by 0.50 and 1.24, respectively. The identification of the actuating force is very important when we consider appropriate application systems. For instance, static mass of the flexible vibrating structures is directly related to the actuating force.

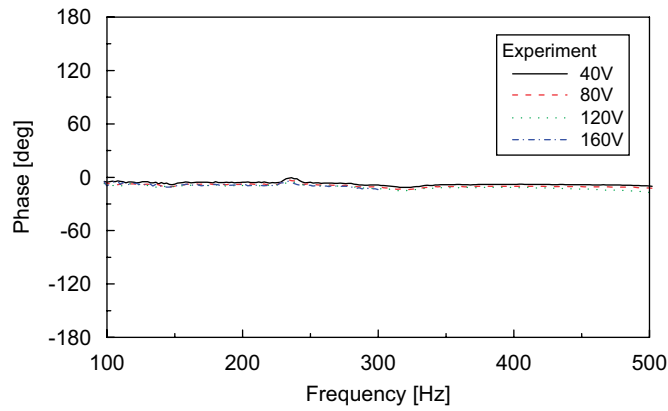


Fig. 6. Time delay of the inertial actuator.

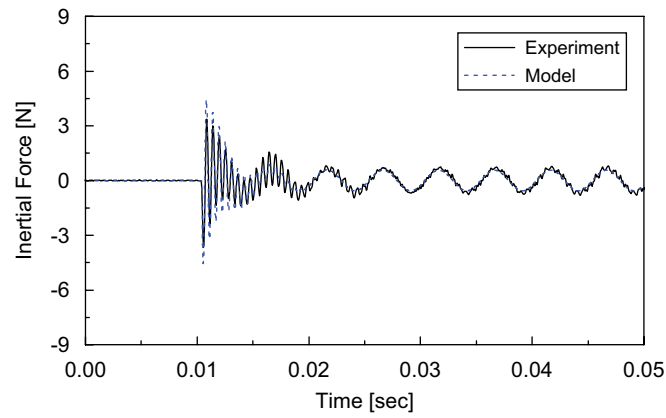


Fig. 7. Time response of the inertial force generated by the inertial actuator.

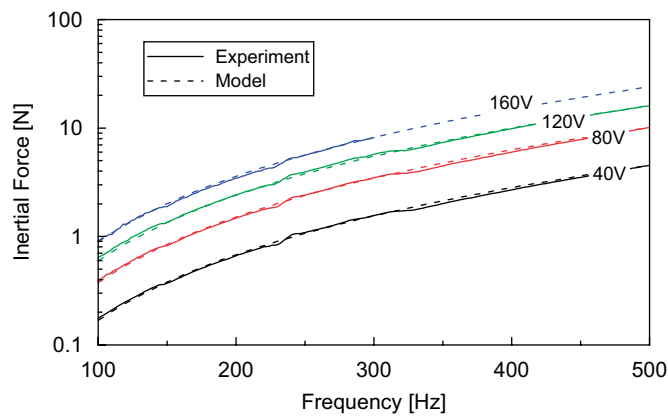


Fig. 8. Frequency responses of the inertial force generated by the inertial actuator.

#### 4. Concluding remarks

In this work, a new type of inertial actuator featuring the piezoceramic stack actuator was devised and its dynamic characteristics are experimentally verified. The proposed inertial actuator consists of the inertial mass

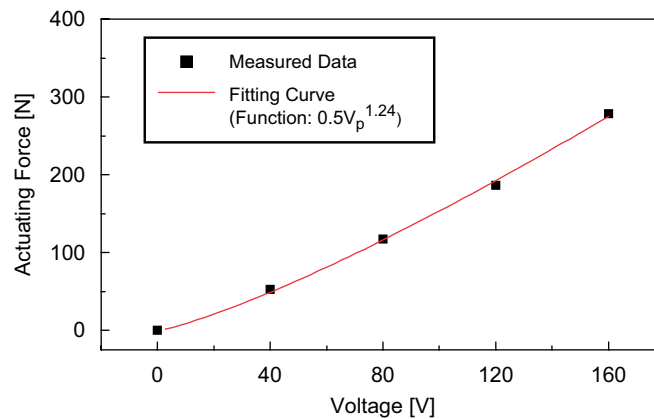


Fig. 9. Identified actuating force of the inertial actuator.

on the top of the piezoceramic stack, the pre-stress spring and housing. After experimentally evaluating the voltage-dependent displacement and force of the piezoceramic actuator, a mathematical model of the inertial actuator was derived. A comparative work on the inertial force between experiment and prediction has been undertaken showing the validity of the proposed dynamic model. In addition, actuating force of the inertial mount has been identified in exponential form. It is finally remarked that application of the proposed inertial actuator to the inertial mount for the vibration control of flexible structures will be explored as a second phase of this preliminary study.

### Acknowledgment

This work was supported by Inha University Research Grant. This financial support is gratefully acknowledged.

### References

- [1] A. Baz, S. Poh, Performance of an active control system with piezoelectric actuators, *Journal of Sound and Vibration* 126 (2) (1988) 327–343.
- [2] S.B. Choi, J.H. Hwang, Structural vibration control using shape memory actuators, *Journal of Sound and Vibration* 231 (4) (2000) 1168–1174.
- [3] S.B. Choi, Vibration control of a flexible structure using ER dampers, *Journal of Dynamic Systems, Measurement and Control* 121 (1996) 134–138.
- [4] I. Bruant, G. Coffignal, F. Léné, M. Vergé, Active control of beam structures with piezoelectric actuators and sensors: modeling and simulation, *Smart Materials and Structures* 10 (2001) 404–408.
- [5] C.L. Davis, G.A. Lesieutre, An actively tuned solid-state vibration absorber using capacitive shunting of piezoelectric stiffness, *Journal of Sound and Vibration* 232 (3) (2000) 601–617.
- [6] M.S. Tsai, K.W. Wang, Control of a ring structure with multiple active passive hybrid piezoelectrical networks, *Smart Materials and Structures* 5 (1996) 695–703.
- [7] T. Kamada, T. Fujita, T. Hatayama, T. Arikabe, N. Murai, S. Aizawa, K. Tohyama, Active vibration control of frame structures with smart structures using piezoelectric actuators (vibration control by control of bending moments of columns), *Smart Materials and Structures* 6 (1997) 448–456.
- [8] A. Premont, J. Dufour, C. Malékian, Active damping by a local force feedback with piezoelectric actuators, *Journal of Guidance, Control, and Dynamics* 15 (2) (1992) 390–395.
- [9] M.D. Jenkins, P.A. Nelson, S.J. Elliott, Active isolation of periodic machinery vibrations FORM resonant structures, *American Society of Mechanical Engineers Winter Annual Meeting—Active Noise and Vibration Control*, Vol. NCA-8, Dallas, TX, 1990, pp. 95–99.
- [10] T. Ushijima, K. Takano, H. Kojima, High performance hydraulic mount for improving vehicle noise and vibration, SAE Technical Paper Series 880073, 1988.



- [11] S.B. Choi, S.H. Kim, S.R. Hong, Vibration isolation of beam structure using hybrid mount associated with rubber and piezoactuator, *Proceedings of the SPIE* 5056 (2003) 241–246.
- [12] K. Mitsuhashi, T. Biwa, S. Mizuhara, K. Sugiura, K. Ogata, N. Nakai, Application of active vibration isolating system to diesel engine mounting, *CIMAC Proceedings of the International Congress on Combustion Engines*, Vol. 1, 1989, pp. 281–300.
- [13] G.A. Lesieutrea, R. Rusovicib, G.H. Koopmannc, J.J. Dosch, Modelling and characterization of a piezoceramic inertial actuator, *Journal of Sound and Vibration* 261 (2003) 93–107.
- [14] IEEE Standard on Pizelectricity, ANSI/IEEE Std., 1987.